CARBON letters

Note

Carbon Letters Vol. 21, 93-97 (2017)

Green synthesis of reduced graphene oxide using ball milling

G. Calderón-Ayala[1], M. Cortez-Valadez[2,*], P. G. Mani-Gonzalez[3], R. Britto Hurtado[1], J. I. Contreras-Rascón[4], R. C. Carrillo-Torres[4], Ma. E. Zayas[1], S. J. Castillo[1], A. R. Hernández-Martínez[5] and M. Flores-Acosta[1]

[1]Departamento de Investigación en Física, Universidad de Sonora, Apdo. Postal 5-88, 83190, Hermosillo, México
[2]CONACYT-Departamento de Investigación en Física, Universidad de Sonora, Apdo. Postal 5-88, 83190, Hermosillo, México
[3]Instituto de Ingeniería y Tecnología, Departamento de Física y Matemáticas, Universidad Autónoma de Ciudad Juárez, Cd. Juárez 32310, México
[4]Departamento de Física, Universidad de Sonora, Apdo. Postal 5-88, 83190, Hermosillo, México
[5]Centro de Física Aplicada y Tecnología Avanzada (CFATA), Universidad Nacional Autónoma de México Campus Juriquilla, Querétaro 76130, México

Article Info
Received 13 April 2016
Accepted 25 October 2016

***Corresponding Author**
E-mail: jose.cortez@unison.mx
Tel: +52-662-289-3792

Open Access
DOI: http://dx.doi.org/10.5714/CL.2017.21.093

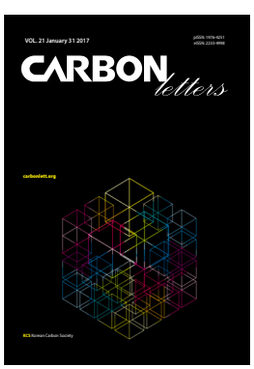

http://carbonlett.org

pISSN: 1976-4251
eISSN: 2233-4998

Today, finding superior methods for synthesis of graphene oxide (GO) and reduced graphene oxide (rGO) from commercial graphite, is still a challenge. The global industry requires the use of synthesis methods that are price-competitive and also use processes that are environmentally compatible. GO is a substrate used for several chemical transformations, including its reduction to related materials, such as rGO and graphene. The rGO has been used recently to increase catalytic activity in the o-nitroaniline reduction to $NaBH_4$ and Raman activity in test molecules as p-aminothiophenol [1]. Other authors showed that the rGO in combination with carbon nanotubes has the properties of supercapacitors [2]. Mao et al. [3] obtained a gas sensor type field defect transistor of high sensitivity at low concentrations, using sheets of rGO. On the other hand, rGO linked with Cu_2O nanocrystals is capable of removing dye pollution from wastewater [4].

An efficient method for synthesizing GO was improved by Hummers et al. [5] in 1958, who used $KMnO_4$ and H_2SO_4. The current synthesis methods are based on modifications and improvements of this method. Among these, the ones to be emphasized are those that use reduction agents (e.g., hydrazine, hydroquinone, sodium borohydride, and ascorbic acid) [5-9].

In new materials synthesis, the search for environmentally friendly methods has motivated several authors to explore the use of bio-reducers obtained from plants, fruits, fungi, and bacteria [10-14].

This has led us to consider, among various options, the *Opuntia ficus-indica* (OFI) plant extract for its significant potential. This plant is a strong reducer and stabilizer used in nanomaterials synthesis. By using this OFI extract, we can dispense with using H_2SO_4, HNO_3, or H_3PO_4; as well as the common oxidants ($KMnO_4$ or $KClO_4$) for rGO synthesis. On the other hand, the plant extract has traces of Mn, Cl, P, K, S, Se, etc. [15]. In this research, we are proposing a green synthesis method by which to generate rGO from commercial graphite, methanol, and OFI extract as reducing agent, in a high energy process of wet ball milling.

Young OFI cladodes were cleaned and separated from the transparent external cuticle. Then, they were cut into small pieces and added to deionized water at 80°C until the color changed from green to yellow (about an hour). Next, the heated solution was passed through a filter containing small pieces of young leaves, to obtain a viscous, whitish solution.

Then, 2.0 mg of commercial graphite (Sigma Aldrich, USA; 99.995% purity level), 1.0 mL of methanol, 2.0 mL of OFI extract, and 40 mL of deionized water were mixed in a beaker. Afterwards, the mixture was put in a zircon oxide vial and subjected to a high energy ball milling (HEBM) process at 250 r/min. This was done intermittently every 30 min for 8 h. Subsequently, 20 mL of a solution of 0.01 M ascorbic acid was added and the milling process continued for 8 h. The mixture changed its tone from black to gray. At the end of the process, samples were dried at room temperature. The synthesis process using high-energy milling

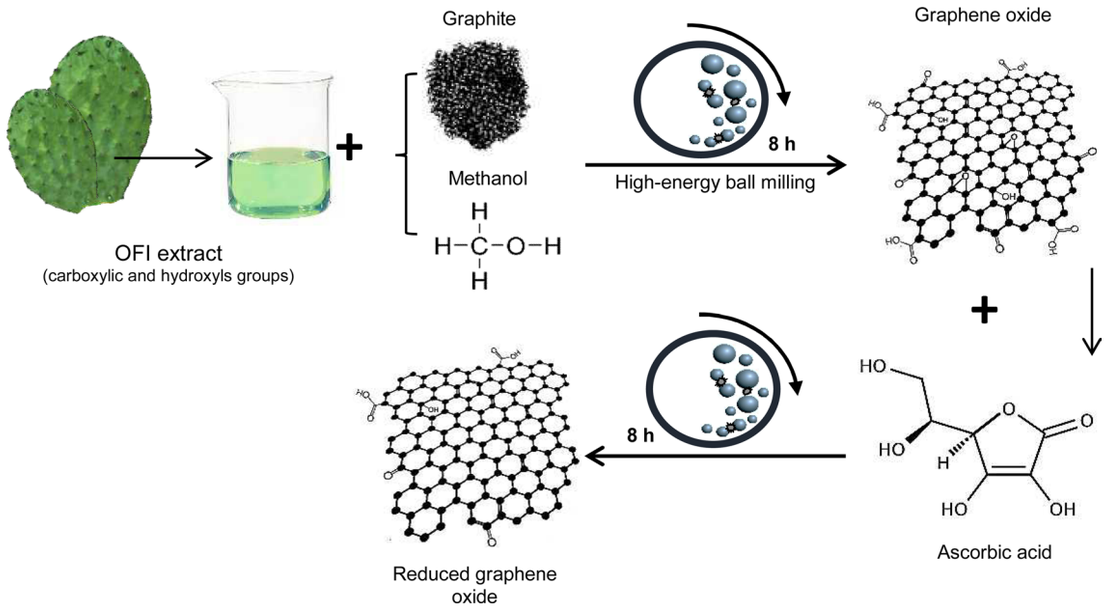

Fig. 1. Green synthesis of reduced graphene oxide by high-energy ball milling. OFI, *Opuntia ficus-indica.*

to obtain rGO, is represented in Fig. 1. Raman spectroscopy of the graphene powder was done using a Horiba Jobin Yvon device (Japan), LabRam HR with laser He-Ne (632.8 nm) at 20–25 mW. The X-ray photoelectron spectroscopy (XPS) measurements were made in a Perkins-Elmer 04-300 device (USA), using MgKa 1×10^{-7} Torr. The transmission electron microscopy (TEM) was done using a JEOL JEM-2010F (Japan). For the last measurements, a solution drop was dispersed on a nickel microgrill, and then placed in a vacuum.

Raman spectroscopy is widely used for characterization of graphite materials. The technique helps to determine the presence of individual, double, and few-layer sheets; as well as the level of disorder in the hexagonal, bi-dimensional symmetry, and the doping level [16]. The main characteristic Raman bands of graphite, for GO and rGO, are located at about (1350 and 1580) cm^{-1} (bands D and G, respectively). The induced defects (D) band is associated with the breathing modes in the rings with sp^2 hybridization [17]. This band exhibits a proportional shift of location with increase of laser excitation energy (up to 50 cm^{-1}) to higher energy states. The D band also exhibits a significant decrease in intensity in response to excitation energies of about 4 eV [18]. The G band is characteristic of graphite material and is associated with phonon modes with E_{2g} symmetry [19].

The intensity ratio between those bands allows distinction between the different kinds of graphite materials [20]. Fig. 2a shows the Raman spectroscopy results for commercial graphite. The G band has greater relative intensity than the D band. The milling process promotes graphite fracture, yielding a nanostructured material that provides an advantage for exfoliation. We supposed that several molecules from the plant extract had the tendency to be intercalated slightly between graphene layers in this stage. Because the oxidation processes have an initial stage in the layer edges [21], the HEBM reduces the interaction area of the graphene compounds promoting these oxidation processes. After 8 h of milling, an important decrease of the G band intensity was observed (Fig. 2b), with respect to the one obtained of commercial graphite (Fig. 2a). We suppose that, this is consequence of a temporal oxidation stage of the graphite sheets after their interaction with methanol, and the carboxylic and hydroxyl groups in the components of the OFI extract. This could be because, in this stage, starch, sucrose, and fructose components (carboxylic groups and hydroxyls) have been fragmented and attached to several carbon layers due to the HEBM, showing a certain oxidation level (Fig. 2b).

After incorporation of the ascorbic acid and 8 h of additional milling, a G-band decrease was observed to a relative intensity lower than the D band (Fig. 2c). This could be explained by the presence of rGO, due to the commercial ascorbic acid that favors the reduction process. Park et al. [22] said that the reduction process could start in the graphene layers in ways similar to the oxidation process. Continuing with milling process increased the interaction area between the ascorbic acid and the GO layers, promoting the synthesis of rGO. The D band presents a relative intensity greater than the G band of rGO in Fig. 2c. This is consistent with reports by Cui et al. [23], Fan et al. [24], and Ding et al. [25].

XPS was used to analyze the chemical graphene species. GO (not shown) and rGO results were also obtained using Raman spectroscopy. Both techniques are useful to determine and corroborate the chemical environment and vibrational modes, respectively, of atoms. Fig. 3 shows the carbon 1s core level spectra with five signals that were fitted. The C 1s spectra were de-convoluted, and indicate different oxygen functional groups on the rGO structure.

The signal at 284.4 eV was associated with C-C covalent bonds. The signal at 285.5 eV was related to C-N covalent bonds. The signal at 286.5 eV was attributed to hydroxyl bonds (C-OH). The ratio between the intensity of C-C and C-O signals

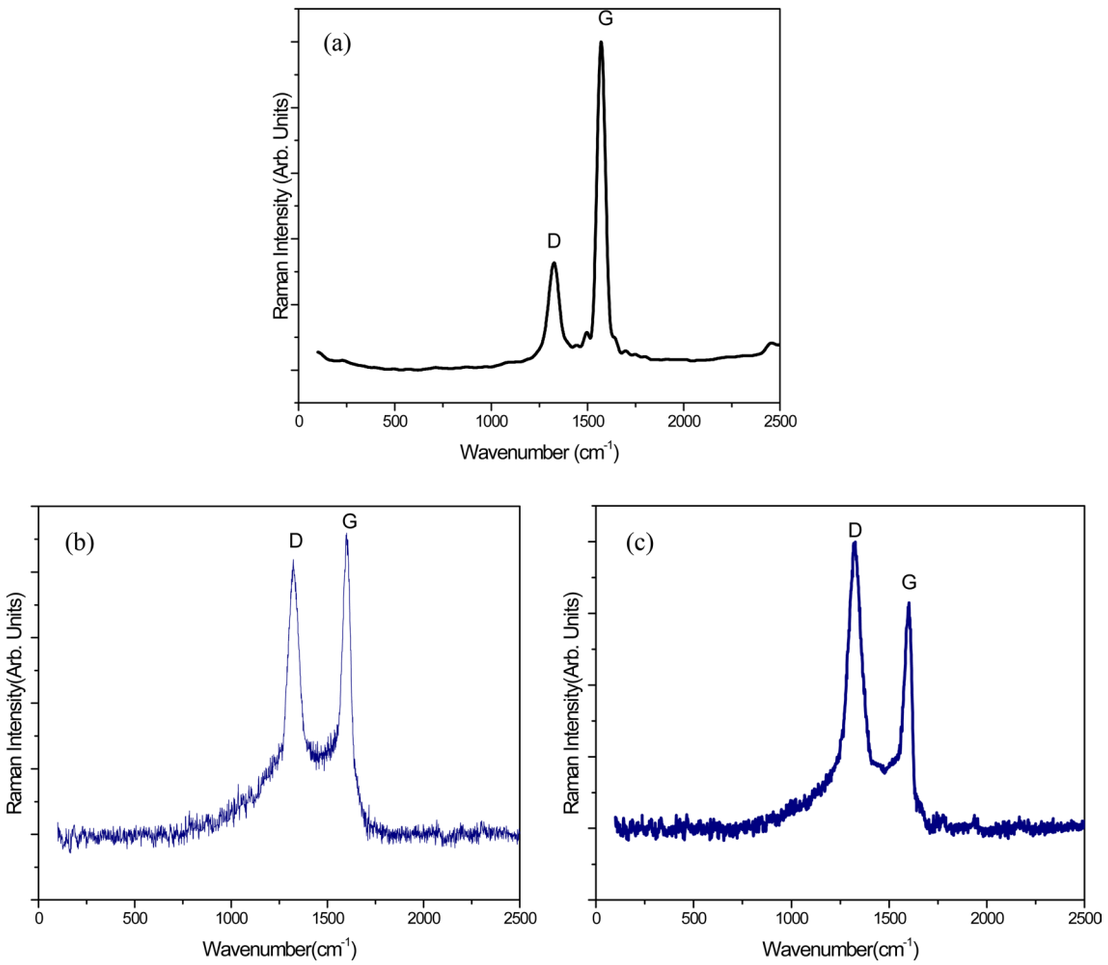

Fig. 2. Raman spectra of (a) graphite, (b) graphene oxide, and (c) reduced graphene oxide.

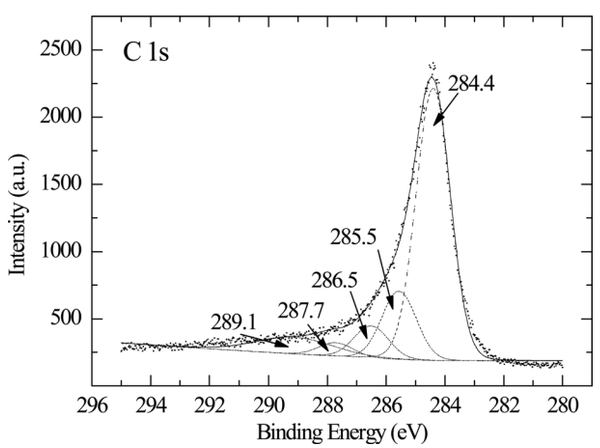

Fig. 3. X-ray photoelectron spectroscopy spectra of reduced graphene oxide.

was 8.5. This ratio suggests the presence of an rGO structure comparable with the results obtained by Fan et al. [24]. The signal at 287.7 eV corresponds to epoxy bonds (C=O) and the signal at 289.1 eV was associated with carbonyl bonds (COO).

After the HEBM process, TEM microscopy was used to study structural and dimensional properties of the materials obtained. TEM microscopy allows analysis of the material morphology at nano-metric scale, even to a few Angstroms. The TEM images show sheet carbon nanostructures on the order of 0.68 nm (2 layers) and 3.7 nm (11 layers) thick (observable in Fig. 4a), and around 20 nm long in the latter case. The interplanar distance measured allows identification of the crystalline planes associated with graphene (3.41 Å). This is similar to the experimental value reported by Pendolino et al. [26] (3.40 Å corresponding to the [1 0 1] plane), obtained after dispersing graphene in methanol.

In Fig. 4b and c, laminar structures are shown that are 75–100 nm long. Due to the tonality of the laminar material in Fig. 4c, we can assume that there are only a few layers of rGO. These results confirm the efficiency of the synthesis process using OFI plant extract as a powerful exfoliator, and ascorbic acid as an efficient reducer of GO sheets, combined with HEBM.

In addition to the fraction of graphite reduced during the HEBM process, the reduction process was favored by the wet medium and external temperature of about 50°C, during synthe-

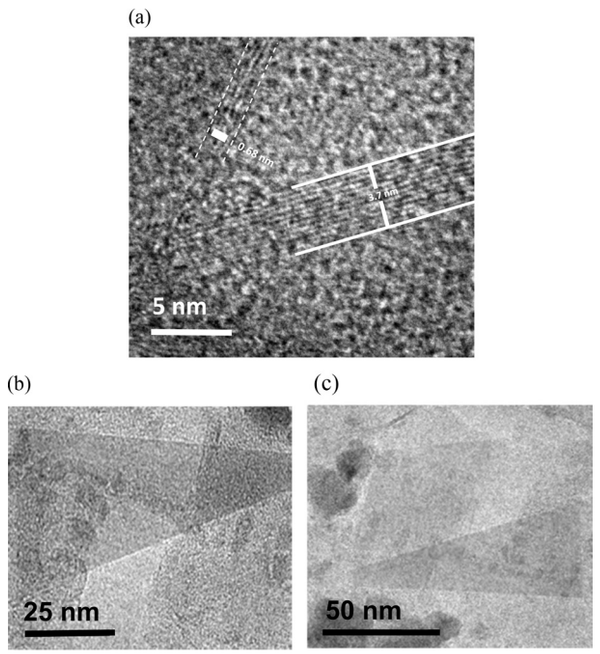

Fig. 4. Transmission electron microscopy image of some reduced graphene oxide sheets: (a) side view and (b, c) top views.

sis of nanostructured materials using OFI extract [27].

In consequence, this extract is a competitive green alternative for obtaining nanostructured materials for the reduction of a few graphene sheets without the use of acids like HCl or H_2SO_4 [28]. From these promising results, it seems that this process could be used to reduce manufacturing costs for devices such as transparent conductors, electronic conveyors, and molecular sensors; for which rGO has recently been used [28-30].

A proposal for obtaining a few layers of rGO employing green synthesis using the OFI plant extract and HEBM was herein presented.

From characterization of the material synthesized, we found the locations of the Raman bands and relative intensity associated with the D and G bands, and they correspond to those previously reported. This confirms the presence of laminar material a few nanometers thick (after HEBM). The XPS spectra confirmed the reduction of the GO by identifying the bands: 286.5 eV (C-O), 287.8 eV (C=O), and 289.1 eV (C(O)O). The TEM microscopy images confirmed the presence of nanostructured material 0.68 nm thick, and 75–100 nm long.

Our results show that our process represents a potential alternative for synthesis of a few layers of rGO at industrial scale, due to its low environmental impact and low cost of production. It could be used to reduce manufacturing costs for the devices already mentioned and others in the health area.

Acknowledgments

Special thanks to the support given by “Laboratorio de Microscopía electrónica de Transmisión del Departamento de Física de la Universidad de Sonora”

Conflict of Interest

No potential conflict of interest relevant to this article was reported.

References

[1] Huang J, Zhang L, Chen B, Ji N, Chen F, Zhang Y, Zhang Z. Nanocomposites of size-controlled gold nanoparticles and graphene oxide: formation and applications in SERS and catalysis. Nanoscale, **2**, 2733 (2010). https://doi.org/10.1039/C0NR00473A.

[2] Dong X, Xing G, Chan-Park MB, Shi W, Xiao N, Wang J, Yan Q, Sum TC, Huang W, Chen P. The formation of a carbon nanotube–graphene oxide core–shell structure and its possible applications. Carbon, **49**, 5071 (2011). https://doi.org/10.1016/j.carbon.2011.07.025.

[3] Mao S, Yu K, Cui S, Bo Z, Lu G, Chen J. A new reducing agent to prepare single-layer, high-quality reduced graphene oxide for device applications. Nanoscale, **3**, 2849 (2011). https://doi.org/10.1039/C1NR10270B.

[4] Li B, Cao H, Yin G, Lu Y, Yin J. Cu_2O@reduced graphene oxide composite for removal of contaminants from water and supercapacitors. J Mater Chem, **21**, 10645 (2011). https://doi.org/10.1039/C1JM12135A.

[5] Hummers WS Jr, Offeman RE. Preparation of graphitic oxide. J Am Chem Soc, **80**, 1339 (1958). https://doi.org/10.1021/ja01539a017.

[6] Brodie BC. Sur le poids atomique du graphite. Ann Chim Phys, **59**, 466 (1860).

[7] Staudenmaier L. Verfahren zur Darstellung der Graphitsäure. Ber Deut Chem Ges, **31**, 1481 (1898). https://doi.org/10.1002/cber.18980310237.

[8] Dreyer DR, Park S, Bielawski CW, Ruoff RS. The chemistry of graphene oxide. Chem Soc Rev, **39**, 228 (2010). https://doi.org/10.1039/B917103G.

[9] Park S, Ruoff RS. Chemical methods for the production of graphenes. Nat Nanotechnol, **4**, 217 (2009). https://doi.org/10.1038/nnano.2009.58.

[10] Chettri P, Vendamani VS, Tripathi A, Pathak AP, Tiwari A. Self assembly of functionalised graphene nanostructures by one step reduction of graphene oxide using aqueous extract of Artemisia vulgaris. Appl Surf Sci, **362**, 221 (2016). https://doi.org/10.1016/j.apsusc.2015.11.231.

[11] Wang R, Yao Y, Shen M, Wang X. Green synthesis of Au@Ag nanostructures through a seed-mediated method and their application in SERS. Colloids Surf A Physicochem Eng Aspects, **492**, 263 (2016). https://doi.org/10.1016/j.colsurfa.2015.11.076.

[12] Sathishkumar G, Pradeep KJ, Vignesh V, Rajkuberan C, Jeyaraj M, Selvakumar M, Rakhi J, Sivaramakrishnan S. Cannonball fruit (Couroupita guianensis, Aubl.) extract mediated synthesis of gold nanoparticles and evaluation of its antioxidant activity. J Mol Liq, **215**, 229 (2016). https://doi.org/10.1016/j.molliq.2015.12.043.

[13] Navyatha B, Kumar R, Nara S. A facile method for synthesis of gold nanotubes and their toxicity assessment. J Environ Chem Eng, **4**, 924 (2016). https://doi.org/10.1016/j.jece.2015.12.033.

[14] Sawle BD, Salimath B, Deshpande R, Bedre MD, Prabhakar BK, Venkataraman A. Biosynthesis and stabilization of Au and Au–Ag alloy nanoparticles by fungus, Fusarium semitectum. Sci Tech-

nol Adv Mater, **9**, 035012 (2008). https://doi.org/10.1088/1468-6996/9/3/035012.

[15] Tesoriere L, Butera D, Pintaudi AM, Allegra M, Livrea MA. Supplementation with cactus pear (Opuntia ficus-indica) fruit decreases oxidative stress in healthy humans: a comparative study with vitamin C1,2,3. Am J Clin Nutr, **80**, 391 (2004).

[16] Niilisk A, Kozlova J, Alles H, Aarik J, Sammelselg V. Raman characterization of stacking in multi-layer graphene grown on Ni. Carbon, **98**, 658 (2016). https://doi.org/10.1016/j.carbon.2015.11.050.

[17] Ferrari AC, Robertson J. Interpretation of Raman spectra of disordered and amorphous carbon. Phys Rev B, **61**, 14095 (2000). https://doi.org/10.1103/PhysRevB.61.14095.

[18] Pócsik I, Hundhausen M, Koós M, Ley L. Origin of the D peak in the Raman spectrum of microcrystalline graphite. J Non-Cryst Solids, **227-230**, 1083 (1998). https://doi.org/10.1016/S0022-3093(98)00349-4.

[19] Ferrari AC. Raman spectroscopy of graphene and graphite: disorder, electron–phonon coupling, doping and nonadiabatic effects. Solid State Commun, **143**, 47 (2007). https://doi.org/10.1016/j.ssc.2007.03.052.

[20] Seredych M, Idrobo JC, Bandosz TJ. Effect of confined space reduction of graphite oxide followed by sulfur doping on oxygen reduction reaction in neutral electrolyte. J Mater Chem A, **1**, 7059 (2013). https://doi.org/10.1039/C3TA10995J.

[21] Takashiro JI, Kudo Y, Hao SJ, Takai K, Futaba DN, Enoki T, Kiguchi M. Preferential oxidation-induced etching of zigzag edges in nanographene. Phys Chem Chem Phys, **16**, 21363 (2014). https://doi.org/10.1039/C4CP02678K.

[22] Park S, An J, Potts JR, Velamakanni A, Murali S, Ruoff RS. Hydrazine-reduction of graphite- and graphene oxide. Carbon, **49**, 3019 (2011). https://doi.org/10.1016/j.carbon.2011.02.071.

[23] Cui P, Lee J, Hwang E, Lee H. One-pot reduction of graphene oxide at subzero temperatures. Chem Commun **47**, 12370 (2011). https://doi.org/10.1039/C1CC15569E.

[24] Fan J, Wang K, Wei T, Yan J, Song L, Shao B. An environmentally friendly and efficient route for the reduction of graphene oxide by aluminum powder. Carbon, **48**, 1686 (2010). https://doi.org/10.1016/j.carbon.2009.12.063.

[25] Ding YH, Zhang P, Zhuo Q, Ren HM, Yang ZM, Jiang Y. A green approach to the synthesis of reduced graphene oxide nanosheets under UV irradiation. Nanotechnology, **22**, 215601 (2011). https://doi.org/10.1088/0957-4484/22/21/215601.

[26] Pendolino F, Capurso G, Maddalena A, Russo SL. The structural change of graphene oxide in a methanol dispersion. RSC Adv, **4**, 32914 (2014). https://doi.org/10.1039/C4RA04450A.

[27] Álvarez RAB, Cortez-Valadez M, Britto-Hurtado R, Bueno LON, Flores-Lopez NS, Hernández-Martínez AR, Gámez-Corrales R, Vargas-Ortiz R, Bocarando-Chacon JG, Arizpe-Chavez H, Flores-Acosta M. Raman scattering and optical properties of lithium nanoparticles obtained by green synthesis. Vib Spectrosc, **77**, 5 (2015). https://doi.org/10.1016/j.vibspec.2015.02.001.

[28] Becerril HA, Mao J, Liu Z, Stoltenberg RM, Bao Z, Chen Y. Evaluation of solution-processed reduced graphene oxide films as transparent conductors. ACS Nano, **2**, 463 (2008). https://doi.org/10.1021/nn700375n.

[29] Gómez-Navarro C, Weitz RT, Bittner AM, Scolari M, Mews A, Burghard M, Kern K. Electronic transport properties of individual chemically reduced graphene oxide sheets. Nano Lett, **7**, 3499 (2007). https://doi.org/10.1021/nl072090c.

[30] Robinson JT, Perkins FK, Snow ES, Wei Z, Sheehan PE. Reduced graphene oxide molecular sensors. Nano Lett, **7**, 3137 (2008). https://doi.org/10.1021/nl8013007.